Transport and Communications Science Journal

GEOMETRICALLY NONLINEAR RESPONSE OF AXIALLY FUNCTIONALLY GRADED BEAMS SUBJECTED TO A MOVING LOAD

Pham Thi Ba Lien

University of Transport and Communications, No 3 Cau Giay Street, Hanoi, Vietnam

ARTICLE INFO

TYPE: Research Article
Received: 27/12/2025
Revised: 12/05/202026
Accepted: 13/05/2026
Published online: 15/05/2026
https://doi.org/10.47869/tcsj.77.4.8

* *Corresponding author*
Email: phamthibalien@utc.edu.vn; Tel: +84 989535691

Abstract. Understanding the dynamic response of the beam under the actions of a moving load is crucial for practical applications. In this study, nonlinear dynamic characteristics of an axially functionally graded (AFG) beam subjected to a moving load has been performed by using the trigonometric shear deformation beam theory and the von-Kármán geometric nonlinearity. The Voigt model is used to calculate the material properties of the beam. The system of nonlinear differential equation of motion for the beam is derived by using Hamilton's principle. The finite element formula based on the Lagrange and Hermite interpolation functions is employed to discretize the model and obtain a numerical approximation of the system of differential equation of motion in nonlinear analysis. The Newmark method together with the Newton-Raphson iteration method is adopted to solved these equations. To validate the present work, the results in this paper are compared with those of the existing literature and good agreement is achieved. The results show that the power-law index, velocity and moving load magnitude and aspect ratio play a very important role on the beam's nonlinear response.

Keywords: AFG beam, dynamic response, trigonometric shear deformation beam theory, von-Kármán geometric nonlinearity, finite element formula.

1. INTRODUCTION

Research on the dynamics of the beam subjected to moving load has attracted signification attention due to its practical applications in engineering, such as bridges, guideways, railroads, overhead cranes,…This can result in large displacement amplitudes in the beam. Consequently, the linear beam analysis is insufficient to accurately predict the beam'response under moving loads, therefore, the geometric nonlinearity must be considered. It has been shown that the moving load velocity significantly affects on the linear [1-3] and nonlinear dynamic response [4] of the homogeneous beam.

Functionally graded material (FGM), first developed by Japanese scientists in the mid-1984s [5], is a type of material whose properties change continuously within the solid, and thus it overcomes the limitations of traditional composite materials like delamination and stress concentration. Numerous studies have examined the response of FGM beams under moving load, however, most of them focus on the linear behavior. Among these reports, some studies have worked on the FGM beam whose material properties change in beam thickness [6-7], or axial direction [8-12], or both directions [13-15]. Only a few papers have examined the nonlinear response of FGM beams suffering from the external moving load. For instant, Şimşek [16] studied the nonlinear deflections of the beam subjected to moving harmonic load by Timoshenko theory combined with von-Kármán's nonlinear strain–displacement relationships. The beam considered in Ref. [16] has material properties varying continuously in thickness direction by a power law. This report indicated that the beam's nonlinear dynamic responses depend significantly on the material distribution and the moving load velocity. Lohar et al. [17] used the same beam theory to investigate nonlinear response of AFG beam on elastic foundation under harmonic excitation. The beams with different boundary conditions and material properties varying along the beam length were considered on their study. Other related works also can be found in Ref. [18] where Vu and Nguyen studies the nonlinear dynamic behavior of the beam with material properties that vary in both thickness and length under moving load using the third-order shear deformation beam theory.

The objective of this paper to analyze nonlinear dynamic of a simply-supported AFG beam under a moving load is studied. The beam's material properties change continuously along the beam length with a power-law form and are defined by Voigt model. Using the trigonometric shear deformation beam theory together with von-Kármán geometric nonlinearity, the nonlinear differential equations of motion for the AFG beam has been obtained. Finite element formula with the Lagrange and Hermite interpolation expressions is applied to establish the discrete nonlinear motion equations. Nonlinear deflection of the beam is determined by Newmark method together with Newton-Raphson iteration method. The dependence of the nonlinear behavior on the material distribution, moving load velocity, moving load magnitude and the aspect ratio is also examined in detail.

2. AFG BEAM MODEL

An AFG beam is depicted in a Cartesian coordinate system, as shown in Figure 1. The beam has a rectangular cross-section with the width b and thickness h, and is subjected a

moving load P that moves in the axial direction. The velocity of the moving load, *v*, is assumed to be constant.

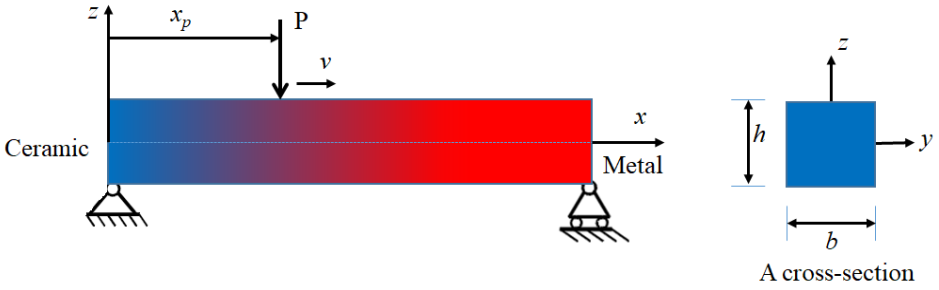

Figure 1. An AFG beam with a moving load.

The volume fractions of ceramic and metal components, V_c and V_m, of the beam are determined as follows [10]

$$V_c = \left(1 - \frac{x}{L}\right)^n, \quad V_c + V_m = 1 \tag{1}$$

where *n* and *L* are, respectively, the power-law index and beam length. According to the Voigt model, the effective property, *P*, can be expressed as follows

$$P = P_c V_c + P_m \left(1 - V_c\right) \tag{2}$$

where P_c and P_m are the properties of ceramic and metal, respectively. From equations (1) and (2), we get

$$P = P_m + \left(P_c - P_m\right)\left(1 - \frac{x}{L}\right)^n \tag{3}$$

3. MATHEMATICAL MODEL

Based on the trigonometric shear deformation beam theory [19], the axial displacement U and transverse displacement W are given by

$$\begin{aligned} U &= u\left(x,t\right) - z w_{,x}\left(x,t\right) + \Psi\left(z\right)\theta\left(x,t\right) \\ W &= w\left(x,t\right) \end{aligned} \tag{4}$$

where $u(x,t)$ and $w(x,t)$ are the axial and transverse displacement of the point on the mid-plane; $\theta(x,t)$ denotes the cross-section rotation; *t* denotes time and $(\ )_{,x}$ indicates the derivative with respect to *x*, and

$$\Psi\left(z\right) = \frac{h}{\pi}\sin\left(\frac{\pi z}{h}\right) \tag{5}$$

Using the assumptions of von-Kármán geometric nonlinearity, the strain-displacement relationship is as follows

$$\begin{aligned}\varepsilon_{xx} &= U_{,x} + \frac{1}{2}W_{,x}^2 = u_{,x} - zw_{,xx} + \Psi\theta_{,x} + \frac{1}{2}w_{,x}^2 \\ \gamma_{xz} &= U_{,z} + W_{,x} = \Psi_{,z}\theta\end{aligned} \tag{6}$$

where ε_{xx} and γ_{xz} are, respectively, axial and shear strain. The constitutive relation for FGM is expressed as

$$\begin{aligned}\sigma_{xx} &= E(x)\varepsilon_{xx} \\ \tau_{xz} &= G(x)\gamma_{xz}\end{aligned} \tag{7}$$

with σ_{xx} and τ_{xz} are the axial and shear stresses, respectively; $G(x) = \dfrac{E(x)}{2\left[1+\nu(x)\right]}$ where elastic modulus E and Poisson's ratio ν are defined from Eq. (3).

The elastic strain energy of the beam U_B is defined by

$$U_B = \frac{1}{2}\int_0^L\int_A \left(\sigma_{xx}\varepsilon_{xx} + \tau_{xz}\gamma_{xz}\right)dAdx \tag{8}$$

with $A=bh$. The elastic strain energy U_B is calculated by summing two parts, $U_B = U^L + U^{NL}$, where U^L and U^{NL} represent the linear and nonlinear effects, respectively. By substituting Eqs. (6) and (7) into Eq. (8), these energy expressions are as follows

$$U^L = \frac{1}{2}\int_0^L \left(A^{11}u_{,x}^2 - 2A^{12}u_{,x}w_{,xx} + A^{22}w_{,xx}^2 + 2A^{13}u_{,x}\theta_{,x} - 2A^{23}w_{,xx}\theta_{,x} + A^{33}\theta_{,x}^2 + B^{33}\theta^2\right)dx \tag{9}$$

and

$$U^{NL} = \frac{1}{2}\int_0^L \left(A^{11}u_{,x}w_{,x}^2 - A^{12}w_{,xx}w_{,x}^2 + A^{13}\theta_{,x}w_{,x}^2 + \frac{1}{4}A^{11}w_{,x}^4\right)dx \tag{10}$$

where the beam rigidities are defined by

$$\begin{aligned}\left(A^{11}, A^{12}, A^{22}, A^{13}, A^{23}, A^{33}\right) &= \int_A E(x)\left[1, z, z^2, \Psi, z\Psi, \Psi^2\right]dA \\ B^{33} &= \int_A G(x)\Psi_{,z}^2 dA\end{aligned} \tag{11}$$

The kinetic energy T of the beam is given by

$$T = \frac{1}{2}\int_0^L\int_A \rho(x)\left(\dot{U}^2 + \dot{W}^2\right)dAdx \tag{12}$$

where the mass density ρ is defined from Eq. (3); $(.)$ presents differentiation with respect to time. Substituting equation (4) into equation (12) yields

$$T=\frac{1}{2}\int_0^L\left[I^{11}\dot{u}^2+I^{11}\dot{w}^2-2I^{12}\dot{u}\dot{w}_{,x}+I^{22}\dot{w}_{,x}^2+2I^{13}\dot{u}\dot{\theta}-2I^{23}\dot{w}_{,x}\dot{\theta}+I^{33}\dot{\theta}^2\right]dx \tag{13}$$

where the mass moments are defined by

$$\left(I^{11},I^{12},I^{22},I^{13},I^{23},I^{33}\right)=\int_A\rho(x)\left[1,z,z^2,\Psi,z\Psi,\Psi^2\right]dA \tag{14}$$

The work of the load *P* at any instant is given below

$$V=-\int_0^L PW(x,t)\delta\left(x-x_P\right)dx \tag{15}$$

where $\delta(.)$ is the Dirac delta function.

Using to Eqs. (9), (10), (13) and (15) in Hamilton's principle, the following nonlinear differential equations of motion for the AFG beam are derived for displacement field (u, w and θ)

$$\begin{aligned}
&\delta u:-\left(I^{11}\ddot{u}-I^{12}\ddot{w}_{,x}+I^{13}\ddot{\theta}\right)+\left(A^{11}u_{,x}-A^{12}w_{,xx}+A^{13}\theta_{,x}+\frac{1}{2}A^{11}w_{,x}^2\right)_{,x}=0\\
&\delta w: I^{11}\ddot{w}-\left(-I^{12}\ddot{u}+I^{22}\ddot{w}_{,x}-I^{23}\ddot{\theta}\right)_{,x}+\left(A^{12}u_{,x}+A^{22}w_{,xx}-\frac{1}{2}A^{12}w_{,x}^2\right)_{,xx}\\
&\qquad-\left(A^{12}u_{,x}w_{,x}-A^{12}w_{,xx}w_{,x}+A^{13}\theta_{,x}w_{,x}+\frac{1}{2}A^{11}w_{,x}^3\right)_{,x}=P\\
&\delta\theta:-\left(I^{13}\ddot{u}-I^{23}\ddot{w}_{,x}+I^{33}\ddot{\theta}\right)+\left(A^{13}u_{,x}+A^{33}\theta_{,x}+\frac{1}{2}A^{13}w_{,x}^2\right)_{,x}-B^{33}\theta=0
\end{aligned} \tag{16}$$

4. SOLUTION METHOD

The finite element method is used herein to discretize the beam's equation of motion. For this purpose, a two-node beam element of length *l* with eight degrees of freedom is considered, and its nodal displacement vector is expressed as

$$\underset{(8\times1)}{\mathbf{d}}=\left[\mathbf{d}_u\quad\mathbf{d}_w\quad\mathbf{d}_\theta\right]^T \tag{17}$$

where the nodal displacement vectors for u,w and θ are calculated at their nodal values as

$$\mathbf{d}_u=\left[u_1\quad u_2\right]^T,\quad \mathbf{d}_w=\left[w_1\quad w_{1x}\quad w_2\quad w_{2x}\right]^T,\quad \mathbf{d}_\theta=\left[\theta_1\quad\theta_2\right]^T \tag{18}$$

The displacement field is interpolated from the nodal displacements as follows

$$u = \mathbf{N}\mathbf{d}_u = \begin{bmatrix} N_1 & N_2 \end{bmatrix} \begin{bmatrix} u_1 \\ u_2 \end{bmatrix}, \quad \theta = \mathbf{N}\mathbf{d}_\theta = \begin{bmatrix} N_1 & N_2 \end{bmatrix} \begin{bmatrix} \theta_1 \\ \theta_2 \end{bmatrix}$$
$$w = \mathbf{H}\mathbf{d}_w = \begin{bmatrix} H_1 & H_2 & H_3 & H_4 \end{bmatrix} \begin{bmatrix} w_1 \\ w_{1x} \\ w_2 \\ w_{2x} \end{bmatrix}, \tag{19}$$

where N_i (i=1,2) and H_j (j=1,…4) are Lagrange and Hermite shape functions, and they are defined as.

$$N_1 = \frac{l-x}{l}, \quad N_2 = \frac{x}{l} \tag{20}$$

and

$$H_1 = 1 - 3\frac{x^2}{l^2} + 2\frac{x^3}{l^3}, \quad H_2 = x - 2\frac{x^2}{l} + \frac{x^3}{l^2},$$
$$H_3 = 3\frac{x^2}{l^2} - 2\frac{x^3}{l^3}, \quad H_4 = -\frac{x^2}{l} + \frac{x^3}{l^2} \tag{21}$$

Based on the above interpolation, the linear and nonlinear strain energy of the beam in Eqs. (9) and (10) are rewritten as

$$U_L = \frac{1}{2}\sum^{nel} \mathbf{d}^T \mathbf{k}^L \mathbf{d}, \quad U_{NL} = \frac{1}{2}\sum^{nel} \mathbf{d}^T \mathbf{k}^{NL} \mathbf{d} \tag{22}$$

where *nel* denotes the number of elements used to discretize the beam; the element linear and nonlinear stiffness matrices, $\mathbf{k}^L$ and $\mathbf{k}^{NL}$ are defined as

$$\underset{8\times8}{\mathbf{k}^L} = \frac{\partial^2 U_L}{\partial \mathbf{d}^2} = \begin{bmatrix} \mathbf{k}_{uu}^L & \mathbf{k}_{uw}^L & \mathbf{k}_{u\theta}^L \\ \left(\mathbf{k}_{uw}^L\right)^T & \mathbf{k}_{ww}^L & \mathbf{k}_{w\theta}^L \\ \left(\mathbf{k}_{u\theta}^L\right)^T & \left(\mathbf{k}_{w\theta}^L\right)^T & \mathbf{k}_{\theta\theta}^L \end{bmatrix} \tag{23}$$

and

$$\underset{8\times8}{\mathbf{k}^{NL}} = \frac{\partial^2 U_{NL}}{\partial \mathbf{d}^2} = \begin{bmatrix} \mathbf{0} & \mathbf{k}_{uw}^{NL} & \mathbf{0} \\ \left(\mathbf{k}_{uw}^{NL}\right)^T & \mathbf{k}_{ww}^{NL} & \mathbf{k}_{w\theta}^{NL} \\ \mathbf{0} & \left(\mathbf{k}_{w\theta}^{NL}\right)^T & \mathbf{0} \end{bmatrix} \tag{24}$$

the sub-matrices in Eqs. (23) and (24) are calculated as follows

$$\begin{aligned}
&\underset{(2\times2)}{\mathbf{k}_{uu}^{N}} = \int_0^l \mathbf{N}_{,x}^T A_{11} \mathbf{N}_{,x} dx, \quad \underset{(2\times4)}{\mathbf{k}_{uw}^{N}} = \int_0^l \mathbf{N}_{,x}^T A_{12} \mathbf{H}_{,x\,x} dx, \quad \underset{(2\times2)}{\mathbf{k}_{u\theta}^{N}} = \int_0^l \mathbf{N}_{,x}^T A_{13} \mathbf{N}_{,x} dx, \\
&\underset{(4\times4)}{\mathbf{k}_{ww}^{N}} = \int_0^l \mathbf{H}_{,xx}^T A_{22} \mathbf{H}_{,x\,x} dx, \quad \underset{(4\times2)}{\mathbf{k}_{w\theta}^{N}} = -\int_0^l \mathbf{H}_{,xx}^T A_{23} \mathbf{N}_{,x} dx, \quad \underset{(2\times2)}{\mathbf{k}_{\theta\theta}^{N}} = \int_0^l \left(\mathbf{N}_{,x}^T A_{33} \mathbf{N}_{,x} + \mathbf{N}^T B_{33} \mathbf{N} \right) dx
\end{aligned} \tag{25}$$

and

$$\begin{aligned}
&\underset{(2\times4)}{\mathbf{k}_{uw}^{NL}} = \int_0^l \mathbf{N}_{,x}^T \mathbf{d}_w^T \mathbf{H}_{,x}^T A_{11} \mathbf{H}_{,x} dx, \quad \underset{(4\times2)}{\mathbf{k}_{w\theta}^{NL}} = \int_0^l \mathbf{H}_{,x}^T \mathbf{d}_w^T \mathbf{H}_{,x}^T A_{13} \mathbf{N}_{,x} dx, \\
&\underset{(4\times4)}{\mathbf{k}_{ww}^{NL}} = \int_0^l \Big(\mathbf{H}_{,x}^T A_{11} \mathbf{N}_{,x} \mathbf{d}_u \mathbf{H}_{,x} - 3\mathbf{H}_{,x}^T \mathbf{H}_{,x} \mathbf{d}_w A_{12} \mathbf{H}_{,xx} \\
&\qquad + \mathbf{H}_{,x}^T \mathbf{N}_{,x} \mathbf{d}_\theta A_{13} \mathbf{H}_{,x} + \frac{3}{2} \mathbf{H}_{,x}^T \mathbf{H}_{,x} \mathbf{H}_{,x}^T \mathbf{H}_{,x} \mathbf{d}_w A_{11} \mathbf{d}_w^T \Big) dx
\end{aligned} \tag{26}$$

Equation (13) is also written as follows

$$T = \frac{1}{2} \sum^{nel} \dot{\mathbf{d}}^T \mathbf{m} \dot{\mathbf{d}} \tag{27}$$

in which the matrix **m** is written as

$$\underset{8\times8}{\mathbf{m}} = \frac{\partial^2 T}{\partial \dot{\mathbf{d}}^2} = \begin{bmatrix} \mathbf{m}_{uu} & \mathbf{m}_{uw} & \mathbf{m}_{u\theta} \\ \left(\mathbf{m}_{uw}\right)^T & \mathbf{m}_{ww} & \mathbf{m}_{w\theta} \\ \left(\mathbf{m}_{u\theta}\right)^T & \left(\mathbf{m}_{w\theta}\right)^T & \mathbf{m}_{\theta\theta} \end{bmatrix} \tag{28}$$

with

$$\begin{aligned}
&\underset{(2\times2)}{\mathbf{m}_{uu}} = \int_0^l \mathbf{N}^T I_{11} \mathbf{N} dx, \quad \underset{(2\times4)}{\mathbf{m}_{uw}} = -\int_0^l \mathbf{N}^T I_{12} \mathbf{H}_{,x} dx, \quad \underset{(2\times2)}{\mathbf{m}_{u\theta}} = \int_0^l \mathbf{N}^T I_{13} \mathbf{N} dx, \\
&\underset{(4\times4)}{\mathbf{m}_{ww}} = \int_0^l \left(\mathbf{H}^T I_{11} \mathbf{H} + \mathbf{H}_{,x}^T I_{22} \mathbf{H}_{,x} \right) dx, \quad \underset{(4\times2)}{\mathbf{m}_{w\theta}} = -\int_0^l \mathbf{H}_{,x}^T I_{23} \mathbf{N} dx, \quad \underset{(2\times2)}{\mathbf{m}_{\theta\theta}} = \int_0^l \mathbf{N}^T I_{33} \mathbf{N} dx
\end{aligned} \tag{29}$$

The work of the load P in equation (15) is rewritten by

$$V = -\sum^{nel} \mathbf{d}^T \mathbf{f}_P \tag{30}$$

where $\mathbf{f}_P$ is element nodal load vector and it is defined as

$$\underset{8\times1}{\mathbf{f}_P} = P \begin{bmatrix} \mathbf{0} \\ \mathbf{H}^T \\ \mathbf{0} \end{bmatrix}_{x_e} \tag{31}$$

where x_e represents the instantaneous position of the load on the element.

Using the derived element matrices, the system of discrete nonlinear equation of motion for the beam are obtained as

$$\mathbf{M}\ddot{\mathbf{D}} + \left[\mathbf{K}^{L} + \mathbf{K}^{NL}(\mathbf{D})\right]\mathbf{D} = \mathbf{F} \tag{32}$$

where $\mathbf{D}$, $\ddot{\mathbf{D}}$ and $\mathbf{F}$ are, respectively, the global nodal displacement, accelerations and load vectors; $\mathbf{M}$, $\mathbf{K}^{L}$ and $\mathbf{K}^{NL}$ denote the global mass, linear stiffness and nonlinear stiffness matrices. The nonlinear equation (32) is solved using Newmark method and Newton-Raphson iteration method.

5. NUMERICAL RESULTS

In numerical results, the nonlinear dynamic deflection of the simply – supported AFG beam is investigated. The dimensions of the beam are: h=0.5 m, b=0.5 m [16] and different values of beam length. The beam material consists of aluminum (Al: E_m=70 GPa, ρ_m=2702 kg/m^3, ν_m=0.3) and zirconia (ZrO_2: E_c=200 GPa, ρ_c=5700 kg/m^3, ν_c=0.3) [16]. The non-dimensional quantities for the dynamic factor (D_d) used here is

$$D_d = \max\left(\frac{w(L/2,t)}{w_{st}}\right) \tag{33}$$

where $w_{st} = PL^3/48E_mI$. The Newmark's method uses a uniform time step $\Delta t = \Delta T/300$, ΔT is the total time that the load P passes through the beam.

Firstly, the accuracy of the present formulation is verified by comparing the results obtained from this paper with those in previous work. For this purpose, the time histories of the mid-span linear deflection of the AFG beam under a moving load obtained in present work is compared with the result of Wang and Wu [10] in Fig. 2, while Fig. 3 compares the curves for the maximum dynamic deflection-moving load velocity of homogeneous beam (n=0) in linear and nonlinear analysis with the results of Şimşek [16]. It is easy to observe the curves in present model agree well with the curves reported by Wang and Wu [10], and Şimşek [16]. Note that the Timoshenko theory combined with Lagrange's equations are used in both Ref. [10] and Ref. [16] to calculate their results.

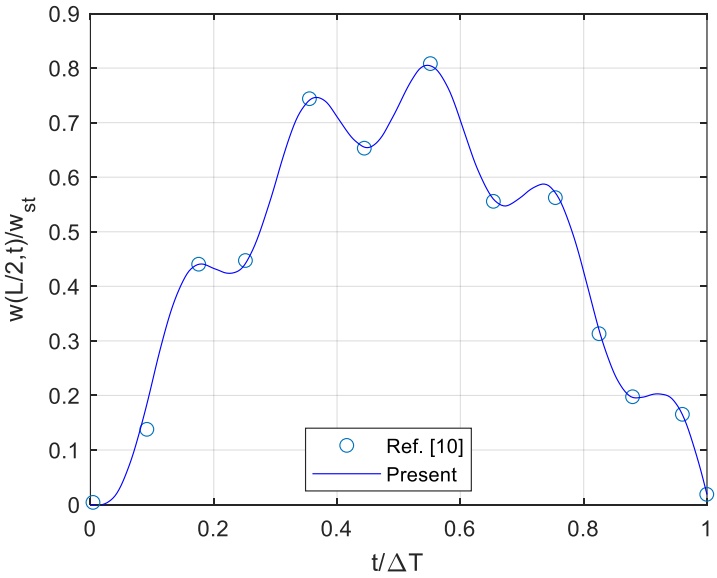

Figure 2. Time histories for the mid-span linear deflections of AFG beam under a moving load for n=0.5, L/h=15, v=50 m/s.

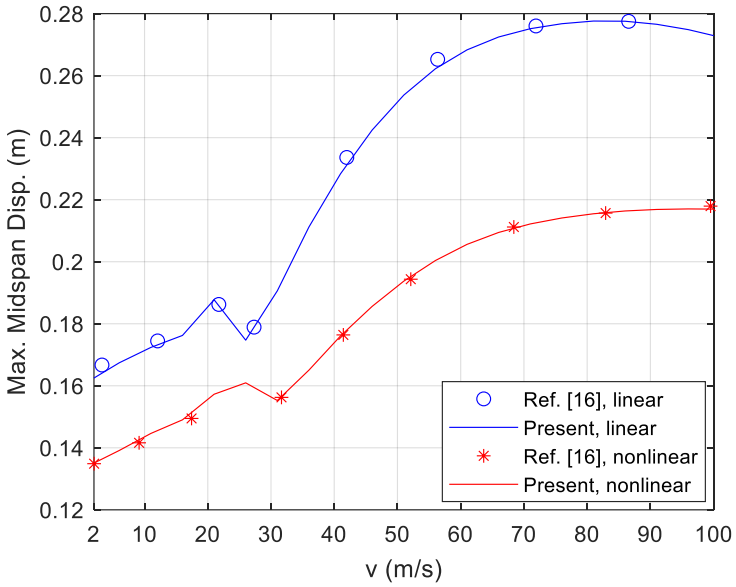

Figure 3. Curves for the maximum dynamic deflection-velocity of the moving load of homogeneous beam subjected to a moving load.

Table 1 shows the convergence study for L/h=10, P=1000 kN, different values of index n and moving load velocity v by calculating the nonlinear dynamic factor of the AFG beam. Irrespective of the values of index n and velocity v, the numerical accuracy is achieved with twenty-four elements. Based on the results in the table, twenty-four elements are used in the subsequent analyses.

Table 1. Convergence of the beam elements in evaluating nonlinear dynamic factor of the AFG beam (L/h=10, P =1000 kN).

v (m/s)	n	*nel*=6	*nel*=12	*nel*=14	*nel*=16	*nel*=18	*nel*=20	*nel*=22	*nel*=24
30	0	1.5110	1.5122	1.5123	1.5123	1.5123	1.5123	1.5122	1.5122
	2	2.9521	2.9557	2.9561	2.9564	2.9566	2.9567	2.9568	2.9568
	5	3.9380	3.9435	3.9443	3.9449	3.9454	3.9457	3.9460	3.9460
60	0	1.5439	1.5429	1.5425	1.5425	1.5424	1.5424	1.5424	1.5424
	2	3.0800	3.0826	3.0825	3.0825	3.0824	3.0821	3.0819	3.0819
	5	4.1514	4.1566	4.1572	4.1572	4.1573	4.1573	4.1573	4.1573

The nonlinear dynamic factor D_d of the AFG beam is shown in table 2 for v=50 m/s, different values of the index n, aspect ratio L/h and moving load magnitude P. Observations from this table show that the index n increasing by increasing in the factor D_d, irrespective of the aspect ratio and magnitude of moving load. This is explained that increases in n will result in a decrease in the percentage of ceramic, as seen from Eq. (1), while the rigidity of ceramic is larger than the metal, hence, the stiffness of the beam decreases, thus the nonlinear dynamic factor increases. It is also observed from table 2 that the beam with L/h=20 yields a lower nonlinear dynamics factor compared to that with L/h=5, irrespective of the index n and magnitude of moving load P. The change in the magnitude of moving load has a significant effect on the nonlinear dynamics factor D_d, the factor D_d increases by increasing the load

magnitude. The dependence of dynamic factor in both linear and nonlinear analysis on the moving load magnitude is more clearly observed in Fig. 4, where the results are calculated L/h=20, v=40 m/s and n={0, 0.5}. Similar to the nonlinear analysis, the linear dynamic factor increases with increasing the magnitude of moving load. On the other hand, the results in Fig. 4 also show that the linear dynamic factor is always higher than the nonlinear dynamic factor, independent of the moving load magnitude and the power-law index n.

Table 2. Nonlinear dynamic factors of the AFG beam for v=50 m/s.

	L/h=5				L/h=20			
P (kN)	n=0.2	n=0.5	n=1	n=3	n=0.2	n=0.5	n=1	n=3
1000	1.8090	2.0781	2.5189	3.7232	1.7276	1.9678	2.3535	3.3313
1500	2.7135	3.1171	3.7783	5.5848	2.5873	2.9449	3.5189	4.9899
2000	3.6180	4.1561	5.0377	7.4462	3.4407	3.9119	4.6657	6.6064
2500	4.5225	5.1951	6.2971	9.3077	4.2834	4.8625	5.7845	8.1595
3000	5.4269	6.2340	7.5565	11.1690	5.1117	5.7926	6.8732	9.6109

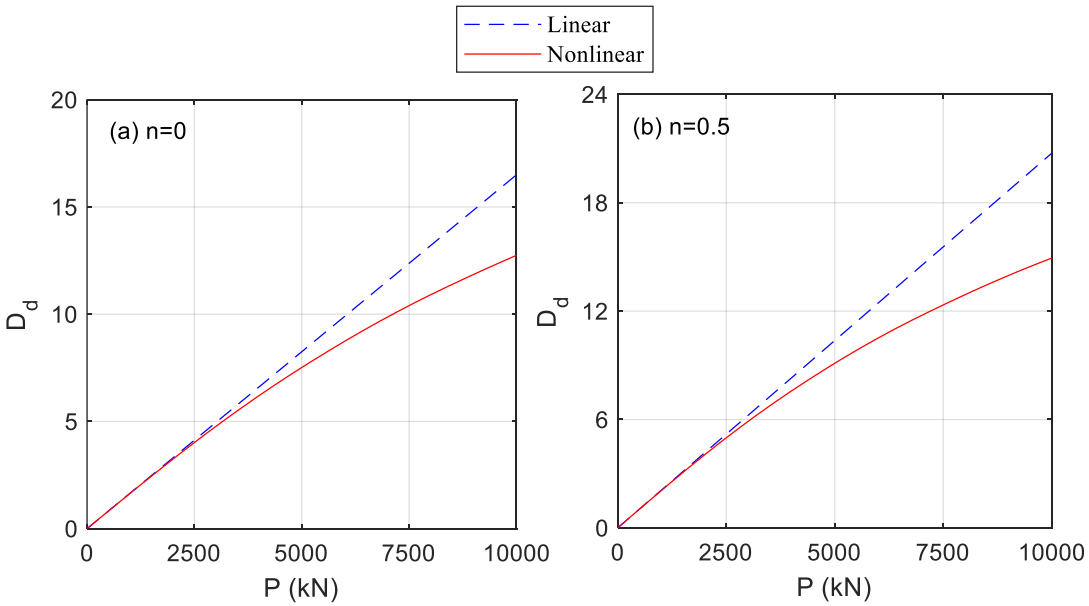

Figure 4 . Variation of linear and nonlinear dynamic factor with magnitude of moving load for L/h=20, v=40 m/s.

The time history curves for the mid-span nonlinear deflection of AFG beam is represented in Fig. 5 for L/h=15, v=50 m/s, P=1000 kN, and n={0, 0.5, 3, 5}. Dependence of the nonlinear deflection on the index n is clearly illustrated in this figure. It is clear that increasing index n results in increasing the nonlinear deflection, regardless of the load positions moving on the beam.

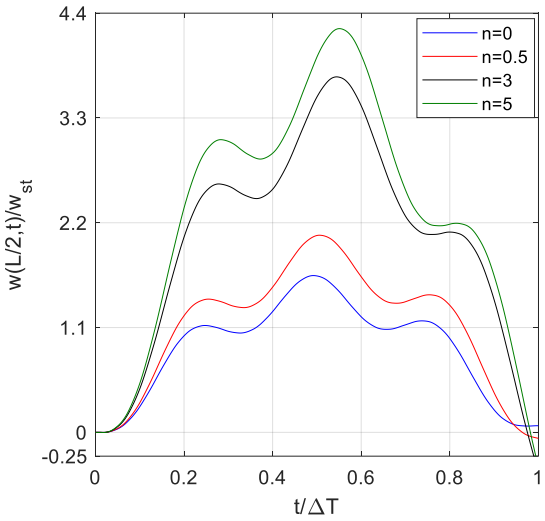

Figure 5. Time histories of mid-span nonlinear deflection for L/h=15, v=50 m/s, P=1000 kN, and the different power-law index.

Figs. 6 and 7 depict the dynamic responses of AFG beam evaluated by the linear and nonlinear analyses. As observed from Fig. 6 for most of the traveling time of moving load, the mid-span deflection predicted by the nonlinear analysis is lower than that predicted by the linear analysis, regardless of different values of the velocity of moving load. A similar trend is observed on the *Dd-v*, as seen in Fig. 7, for L/h=40, P=1000 kN and different values of index n. This is due to the stiffening of the beam in the nonlinear analysis, as seen from Eq. (32). Observing the maximum displacement in Fig. 7 reveals that for the nonlinear case, the maximum response occurs at a higher loading velocity than the linear case, regardless of the values of index n.

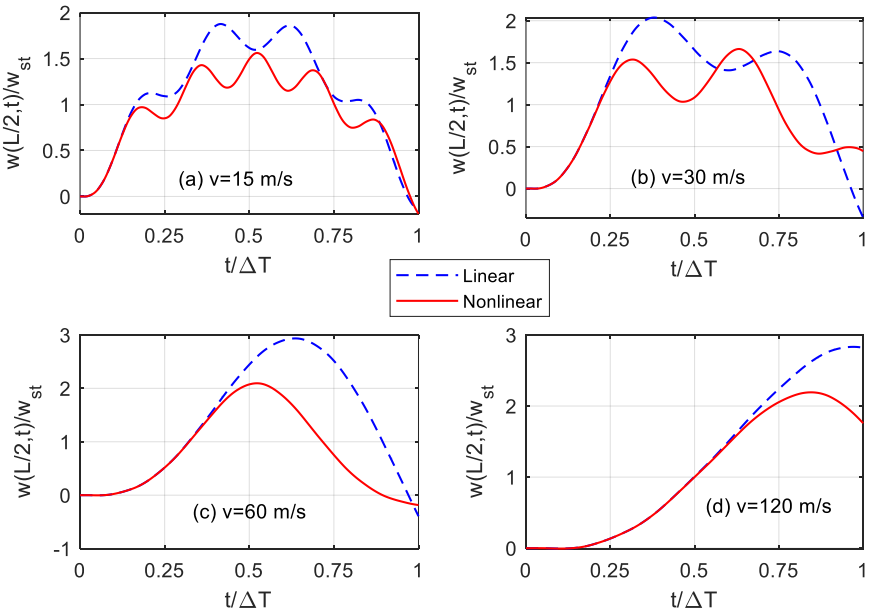

Figure 6. Time histories of mid-span deflection for L/h=40, n=0.5, P=1000 kN, and various moving load velocities.

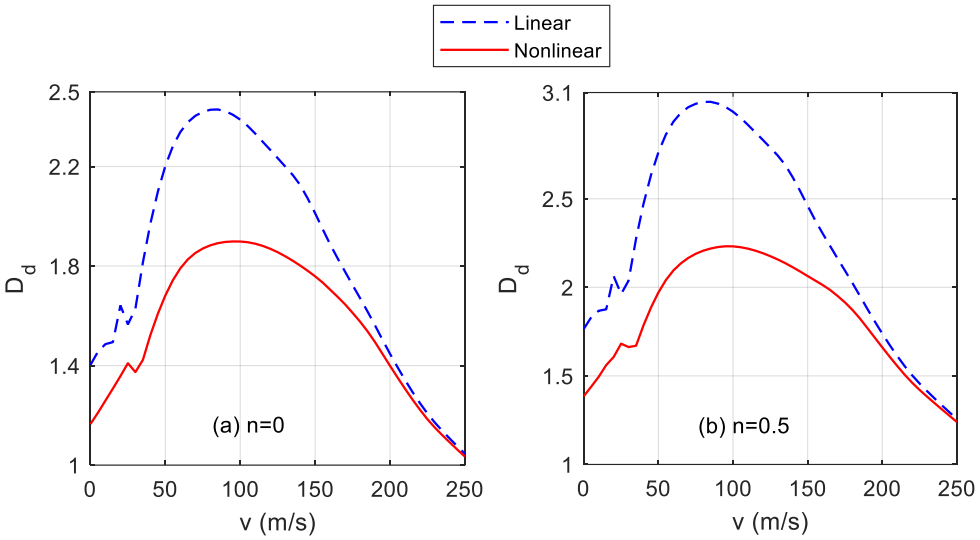

Figure 7. Dynamic factor versus moving load velocity for L/h=40, P=1000 kN.

6. CONCLUSION

In this paper, nonlinear dynamic analysis of a simply-supported AFG beam subjected to a moving load is investigated within the framework of the trigonometric shear deformation beam theory and the von-Kármán geometric nonlinearity. The material properties of the constituent material are deemed to change smoothly along the axial direction by the power-law form. Hamilton's principle is adopted to establish the nonlinear differential equations of motion. This system of equations is then discretized using the finite element method. Numerical solution is obtained by using the Newmark method and Newton-Raphson iteration. The results are the following.

- The linear mid-span deflection is always higher than the nonlinear mid-span deflection, independent of different values of the moving load velocity.
- Irrespective of the values of index n, the nonlinear dynamic factor reaches maximum at higher moving load velocity values compared to linear analysis
- The nonlinear dynamic factor increases with increasing the index n and load P.
- The nonlinear dynamics factor decreases with increasing the aspect ratio, independent of the index n and load P.

ACKNOWLEDGMENT

This research is funded by University of Transport and Communications (UTC) under grant number T2026-CB-012.

REFERENCES

[1]. M. Olsson, On the fundamental moving load problem, Journal of sound and vibration, 145 (1991) 299-307. https://doi.org/10.1016/0022-460X(91)90593-9

[2]. Y. H. Lin, Vibration analysis of Timoshenko beams traversed by moving loads, Journal of Marine Science and Technology, 2 (1994) 4. https://jmstt.ntou.edu.tw/journal/vol2/iss1/4
[3]. H. A. F. A. Santos, A new finite element formulation for the dynamic analysis of beams under moving loads, Computers & Structures, 298 (2024) 107347. https://doi.org/10.1016/j.compstruc.2024.107347
[4]. A. Mamandi, M. H. Kargarnovin, D. Younesian, Nonlinear dynamics of an inclined beam subjected to a moving load, Nonlinear Dynamics, 60 (2010), 277-293. https://doi.org/10.1007/s11071-009-9595-8
[5]. M. Koizumi, FGM activities in Japan, Compos. Part B Eng, 28 (1997) 1–4. https://doi.org/10.1016/S1359-8368(96)00016-9
[6]. S. M. R. Khalili, A. A. Jafari, S. A. Eftekhari, A mixed Ritz-DQ method for forced vibration of functionally graded beams car rying moving loads, Compos Struct, 92 (2010) 2497–2511. https:// doi. org/ 10. 1016/j. comps truct. 2010. 02. 012
[7]. I. Esen, Dynamic response of a functionally graded Timoshenko beam on two-parameter elastic foundations due to a variable velocity moving mass, Int J Mech Sci, 153 (2019) 21–35. https:// doi. org/ 10. 1016/j. ijmec sci. 2019. 01. 033
[8]. M. Şimşek, T. Kocatürk, Ş. D. Akbaş, Dynamic behavior of an axially functionally graded beam under action of a moving harmonic load, Composite Structures, 94 (2012), 2358-2364. https://doi.org/10.1016/j.compstruct.2012.03.020
[9]. B. S. Gan, T. H. Trinh, T. H. Le, D. K. Nguyen, Dynamic response of non-uniform Timoshenko beams made of axially FGM subjected to multiple moving point loads, Structural Engineering and Mechanics, An Int'l Journal, 53 (2015) 981-995. http://dx.doi.org/10.12989/sem.2015.53.5.981
[10]. Y. Wang, D. Wu, Thermal effect on the dynamic response of axially functionally graded beam subjected to a moving harmonic load, Acta Astronautica, 127 (2016) 171-181. https://doi.org/10.1016/j.actaastro.2016.05.030
[11]. A. Ebrahimi-Mamaghani, H. Sarparast, M. Rezaei, On the vibrations of axially graded Rayleigh beams under a moving load, Applied Mathematical Modelling, 84 (2020) 554-570. https://doi.org/10.1016/j.apm.2020.04.002
[12]. V. T. A. Ninh, N. T. K. Khue, Dynamic finite element modeling of axially functionally graded Timoshenko microbeams under a moving mass, Journal of Science and Technology in Civil Engineering (JSTCE)-HUCE, 17 (2023) 128-139. https://doi.org/10.31814/stce.huce2023-17(3)-10
[13]. D. K. Nguyen, Q. H. Nguyen, T. T. Tran, V. T. Bui, Vibration of bi-dimensional functionally graded Timoshenko beams excited by a moving load, Acta Mechanica, 228 (2017) 141-155. https://doi.org/10.1007/s00707-016-1705-3
[14]. A. A. Abdelrahman, M. Ashry, A. E. Alshorbagy, W. S. Abdallah, On the mechanical behavior of two directional symmetrical functionally graded beams under moving load, International Journal of Mechanics and Materials in Design, 17 (2021) 563-586. https://doi.org/10.1007/s10999-021-09547-9
[15]. Q. Zhang, H. Liu, On the dynamic response of porous functionally graded microbeam under moving load, International Journal of Engineering Science, 153 (2020) 103317. https://doi.org/10.1016/j.ijengsci.2020.103317
[16]. M. Şimşek, Non-linear vibration analysis of a functionally graded Timoshenko beam under action of a moving harmonic load, Composite Structures, 92 (2010) 2532-2546. https://doi.org/10.1016/j.compstruct.2010.02.008
[17]. H. Lohar, A. Mitra, S. Sahoo, Nonlinear response of axially functionally graded Timoshenko beams on elastic foundation under harmonic excitation, Curved and Layered Structures, 6 (2019) 90-104.
[18]. A. N. T. Vu, D. K. Nguyen, Nonlinear dynamics of two-directional functionally graded beam under a moving load with influence of homogenization scheme, Journal of Vibration Engineering & Technologies, 12 (2024) 171-185. https://doi.org/10.1007/s42417-024-01409-w
[19]. M. Touratier, An efficient standard plate theory, Int J Eng Sci, 29 (1991) 901–16. https://doi.org/10.1016/0020-7225(91)90165-Y